Wien filter: A wave-packet-shifting device for restoring longitudinal coherence in charged-matter-wave interferometers

Marc Nicklaus* and Franz Hasselbach†
Institut für Angewandte Physik, Universität Tübingen, Auf der Morgenstelle 12, D-7400 Tübingen, Germany
(Received 17 November 1992)

Longitudinal coherence in two-beam interferometers means that the two partial wave packets arrive in the plane of interference simultaneously. In charged-particle interferometers, this simultaneity can be lost due to a difference in the geometrical path lengths, a difference in the optical path length, or a difference in the group velocities for the two wave packets on parts of or all of the beam paths. Several of those influences can combine to yield a net relative spatial delay between the wave packets in the interference plane, thus causing a reduction of the interference fringe contrast. A Wien filter can be used in charged-matter-wave interferometry to compensate for this relative delay and thus to reestablish longitudinal coherence. A Wien filter consists of an electric and a magnetic field perpendicular both to each other and the beam path. In its matched state, i.e., when the electrostatic and the magnetic forces on the electrons exactly cancel each other, the Wien filter neither deflects the beams nor exerts any phase shift on the wave packets. However, wave packets traveling through the Wien filter on laterally separated paths propagate in regions of different electric potentials and in turn with different group velocities, which leads to a longitudinal shift of the wave packets relative to each other. Maximum longitudinal coherence (and thereby fringe contrast) can be restored by choosing the compensating delay caused by the Wien filter exactly opposite to the net relative delay caused by the influences mentioned. An experiment is presented that demonstrates this property of a Wien filter. The coherence-reviving action of a Wien filter is discussed in the context of the incoherent superposition in the registration plane of the plane waves corresponding to different wavelengths in the electron spectrum. It demonstrates that the quantum-mechanical coherence of the self-interfering plane-wave components of the wave packets describing the particle ensemble is more robust than the experimental loss of interference-fringe contrast often suggests. The availability of such a contrast-restoring device is especially important for very-low-energy (a few keV or less) electron interferometry. It is also likely to become important for future ion-beam interferometers.

PACS number(s): 03.65.Bz, 07.80.+x, 41.90.+e

I. INTRODUCTION

The Wien filter, a device used in charged-particle optics, consists of an electric and a magnetic field perpendicular both to each other and to the beam path. It has been put to use in various different ways. The application of a Wien filter as an electron spectrometer [1] or as a device for the conversion of the longitudinal component of the spin direction into a transverse one in electron-polarization experiments is well known [2].

Möllenstedt and Wohland [3] showed that the wave packets in two coherent electron beams are longitudinally shifted relative to each other when they traverse a Wien filter [4] in which the electric and magnetic fields are matched to yield no resultant deflecting force on the electrons. This "matched" mode of operation is defined by the so-called "Wien condition"

$$e\mathbf{E} + e(\mathbf{v} \times \mathbf{B}) = \mathbf{0}. \tag{1}$$

The authors of Ref. [3] used this effect to measure the coherence lengths of electron beams. Their method has been substantially improved in the meantime [5]. It has been refined to the point that it can now be used as a completely new method for measuring electron energy spectra, effectively enabling one to do Fourier spectroscopy of electron waves [6]. In a conceptually similar experiment, Kaiser, Werner, and George [7] measured the longitudinal coherence length of a thermal neutron beam. The effect of chromatic aberration and partial coherence on the interference pattern in electron biprism interferometers was studied theoretically by Lenz and Wohland [8].

In the present paper we want to focus attention on an application of the Wien filter in charged-particle interferometry. We describe its capability of *reestablishing* full longitudinal coherence of the two partial beams. This feature became apparent in the course of a Sagnac experiment [9,10] performed with a new type of low-energy electron biprism interferometer [11], and it proved to be essential for the successful completion of the experiment [12].

This effect of a Wien filter is closely related to what Clothier *et al.* [13] have recently called "phase echo" in a neutron interferometrical experiment. These authors used a sample (a slab placed in one arm of the neutron interferometer) of a material with a negative scattering length to counteract the destructive effect on the lon-

gitudinal coherence of a similar sample made out of a material with a positive scattering length.

The theoretical basis of all those contrast-reestablishing procedures in particle interferometry is the superposition principle, one of the fundamental assumptions in quantum mechanics. It allows one to build a localized wave packet—which follows from the unavoidable energy spread (or equivalently the de Broglie wavelength spread) of particle beams—by a Fourier sum of plane waves, with a (complex) spectrum $a(\mathbf{k})$,

$$\Psi(\mathbf{r},t) = \int a(\mathbf{k})\, e^{i(\mathbf{k}\cdot\mathbf{r}-\omega_k t)} d\mathbf{k}. \tag{2}$$

From this it follows that the individual plane waves are linearly independent and can therefore experimentally be acted upon independently and reversibly. This has very recently been demonstrated in neutron interferometrical experiments where filtering out a narrow energy band in the recombined beam *after* the actual interferometer restored visibility of the interferogram [14], or where narrowing the neutron wavelength spectrum by introducing time slices in the registration process in time-of-flight interferometry conserved fringe visibility even when the contrast disappeared in the overall pulse [15]. Rauch [16] has very recently discussed this "coupling" of coherent wave packets through their constituting narrow plane-wave bands in the context of Einstein-Podolsky-Rosen (EPR) situations and nonlocality in quantum physics.

Klein, Opat, and Hamilton [17] showed that although the spatial extent σ_x of a wave packet increases according to

$$\sigma_x{}^2(t) = \sigma_x{}^2(0) + \left(\frac{\hbar t}{2m\sigma_x(0)}\right)^2 \tag{3}$$

along the beam path due to the inherent dispersion of massive particle beams even in vacuum, the coherence length as it manifests itself in the fringe visibility function in an interferometer remains constant, and is proportional to $\sigma_x(0)$. Throughout this paper, when referring to wave packets anywhere on the beam path, we mean this coherence-length part (or extent) of the wave packets (unless specifically stated otherwise), which could therefore also be called "coherence-length packets."

The basic principles mentioned so far in the context of (massive) particle interferometry are of course equally at work in optical (photon) interferometry, and light optical experiments similar to the ones mentioned above have been performed recently. The dispersion cancellation effect in infrared photon interferometry investigated by Steinberg, Kwiat, and Chiao [18] appears to be the counterpart of the coherence length conservation in particle interferometry. The same authors' observation of a "quantum eraser" [19] demonstrates the possibility of revival of coherence in a two-photon interference experiment.

II. EXPERIMENTAL SETUP

The basic setup of this interferometer is shown in Fig. 1. A diode field emission electron gun illuminates the electron optical biprism [20] coherently. The biprism

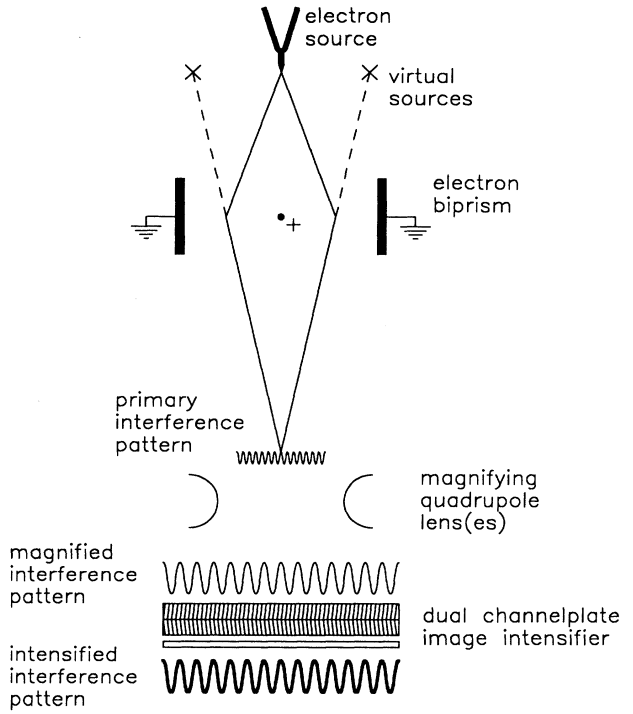

FIG. 1. Basic setup of the interferometer. A diode field-emission source illuminates the biprism filament coherently. The primary interference pattern is magnified by two electrostatic quadrupole lenses and intensified by a dual-stage image intensifier.

splits the electron beam into two partial beams, thus creating two virtual coherent electron sources. The biprism consists of a metallized quartz filament of a diameter in the range between typically 0.5 and 2 μm centered between two grounded electrodes. The two beams overlap behind the biprism filament and form the primary two-beam interference pattern. The spacing s of the interference fringes depends on the angle of superposition γ of the two quasimonochromatic fields of plane waves according to [21]

$$s = \frac{\lambda}{\gamma}, \tag{4}$$

with the de Broglie wavelength $\lambda = h/p$. The angle of superposition and in turn the spacing s can be varied by simply changing the positive potential of the biprism filament.

Field emission extraction voltages between 150 V and 3 kV are used. Even at those low electron energies (no additional acceleration is provided), s is in the submicrometer range due to the short de Broglie wavelength (<1 Å) of the electrons. Therefore the primary image must be magnified. This is accomplished by a two-stage astigmatic electron microscope consisting of two electrostatic quadrupole lenses. The magnified interference image is intensified by two cascaded multichannel plates. It is converted into a visible fringe pattern by a P20 phosphor on a fiber optic plate through which the image is

transferred from the ultrahigh vacuum environment to the laboratory, where it is subject to registration and further evaluation [10]. This setup allows single electrons to be registered with a high quantum detection efficiency of approximately 0.8 [22, 23] for the electron energy range used.

The construction principle of the interferometer, a high precision optical bench to which the electron optical components are rigidly affixed, guarantees an excellent alignment of these components with the optical axis. The details of this design have been described elsewhere [10, 11]. This construction principle guarantees that the field emission tip, the biprism filament, and the optical axis of the magnifying quadrupoles are prealigned automatically within an error of 10 μm. Therefore, no mechanical alignment of the electron optical components during operation is needed. However, fine alignment of the electron beam is still necessary in order to allow control over the positioning of the interference field in the (magnified) field of view. This is achieved with compact electrostatic deflection elements. The entire electron optical setup of the interferometer used in the experiment is depicted in Fig. 1 of the companion paper [10]. For further elaboration of the choices made in the construction of the interferometer as well as for descriptions of the components not explained here, we refer to [11]. It is primarily the electrostatic deflection elements that can cause relative longitudinal shifts of coherent wave packets in low-energy electron interferometry, which is detailed in the following section.

III. LONGITUDINAL SHIFT OF COHERENT ELECTRON WAVE PACKETS

The influence of an electrostatic deflection element on two laterally separated coherent electron wave packets is shown in Fig. 2(a). The wave packets enter the deflection field on paths separated by the distance Δx [24]. In order to achieve the beam alignment, nonzero voltages $\pm U_d$ have to be applied to the deflection plates, U_d typically ranging from a few to a few hundred V. The electric potential at the optical axis of the deflection element is (ideally) zero. Because of their spatial separation Δx, the coherent beams travel through the deflection field in regions differing in their electric potential by

$$\Delta U_d = 2U_d \frac{\Delta x}{D}, \tag{5}$$

where D is the distance between the two plates. Therefore the two beams travel through the deflection element with different group velocities

$$v_{1,2} = v_0 \pm \Delta U_d \sqrt{\frac{e}{8mU_a}} = v_0 \pm \Delta v, \tag{6}$$

where U_a is the acceleration voltage. This results in a relative delay of the two wave packets after they have left the deflection element. The respective deceleration and acceleration of the beams take place in the fringing fields of the deflection elements. Making the approximation that, in (6), $v_0 \gg \Delta v$, we thus conclude that an electrostatic deflection element, apart from its primary

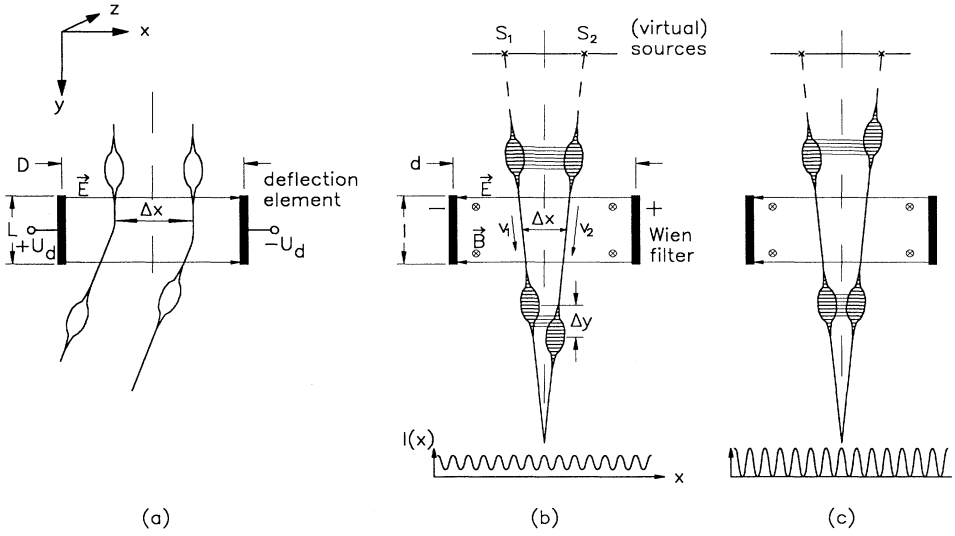

FIG. 2. (a) Influence of an electrostatic deflection element on two electron wave packets laterally separated by Δx. Inside the electrostatic deflection element, the wave packets travel in regions differing in their electric potential. This results in different group velocities and in turn in a relative delay of the two wave packets after they have left the deflection element. (b) Influence of a Wien filter (in its matched state) on two coherent wave packets. The wave packets are shifted longitudinally relative to each other. This reduces overlap of the wave packets in the interference plane, and thereby causes a loss of fringe contrast. The horizontal lines between the wave packets symbolize the fact that the phases remain fixed while the wave packets are shifted in space (see text). (c) Restoration of maximal overlap of coherent wave packets that have experienced a previous longitudinal shift relative to each other. Maximum fringe contrast is reestablished.

purpose of deflecting the beams, has the additional effect on two *spatially separated* electron beams of introducing a longitudinal shift

$$\Delta y = \frac{L}{D}\frac{\Delta x}{U_a}U_d \tag{7}$$

of the two wave packets relative to each other. L is the length of the deflection element. As a result, the wave packets will no longer overlap completely in the observation plane and the fringe contrast is reduced from the maximum value it had at full overlap.

The coherence length is defined as

$$l_c := a\frac{1}{\Delta k} = a\frac{\lambda^2}{\Delta\lambda}. \tag{8}$$

The numerical factor a in (8) is on the order of 1. Its value depends on the exact form of the spectral distribution of the electrons and on the coherence length definition used [25]. Its exact value is of no interest for the problem discussed here. We want to express l_c in experimental parameters, i.e., the acceleration voltage U_a and the voltage uncertainty ΔU corresponding to the energy spread [spectral full width at half maximum (FWHM)] of the electron beam. Since from $\lambda = h/p$ follows

$$\lambda(U_a) = \frac{h}{\sqrt{2me}}\frac{1}{\sqrt{U_a}} \tag{9}$$

for nonrelativistic electrons, we obtain for small values of $\Delta\lambda$

$$\Delta\lambda = -\frac{\lambda}{2U_a}\Delta U. \tag{10}$$

For the sake of convenience, we drop the negative sign and henceforth assume all values to be positive. Combining (8) and (10), we obtain

$$l_c = 2a\lambda\frac{2U_a}{\Delta U}, \tag{11}$$

and using (9) we finally obtain

$$l_c = \frac{2ah}{\sqrt{2me}}\frac{U_a^{1/2}}{\Delta U}. \tag{12}$$

The only significant contribution in our experiment to ΔU was the natural energy spread of the field emission process of 0.3–0.4 eV. In general, less stable acceleration voltages may contribute an additional or even the major part of the energy spread of the electron beam. If a thermionic electron source is used, the energy spread given by the emission process is 1 eV or more. For the energy range used in our interferometer [in the following, (electron) energies and the corresponding (e.g., acceleration) voltages are used interchangeably], U_a = 150–3000 V, and for ΔU = 0.3–0.4 V, the coherence lengths fall in the range between 10 nm and 1000 nm. As the longitudinal shift Δy reaches the order of the coherence length, the contrast of the interference fringes falls off to zero.

The sensitivity of the interferometer to this type of fringe contrast loss increases with decreasing electron energy eU_a. To show this, we derive the voltage U_d' (applied to a deflection element) that is necessary to introduce a longitudinal shift Δy equal to the coherence length l_c. This condition,

$$\Delta y = l_c, \tag{13}$$

is evaluated by combining (7) and (12) to yield

$$U_d' = \frac{2h}{\sqrt{2me}}\frac{a\,D}{L\,\Delta x\,\Delta U}U_a^{3/2}. \tag{14}$$

The decisive point here is the dependency

$$U_d' \propto U_a^{3/2}. \tag{15}$$

In contrast hereto, the deflection voltage U_d'' necessary to produce a given deflection obeys the electrostatic principle, and from this follows

$$U_d'' \propto U_a. \tag{16}$$

The sensitivity of the interferometer to the effect of the longitudinal wave-packet shift can be defined as

$$\eta_l := \frac{U_d''}{U_d'}, \tag{17}$$

and η_l therefore depends on U_a as

$$\eta_l \propto U_a^{-1/2}. \tag{18}$$

This result is readily understood as the combined effects of the decreasing coherence length and the increasing time spent by the wave packets in the deflection field as U_a decreases.

If more than one deflection element is used in the beam path, the longitudinal shifts produced by the individual elements add up linearly. The fringe contrast in the observation plane is then given by the net longitudinal shift resulting from the combined influence of all elements. It should be noted that any electrostatic electron optical element exerts this type of influence on coherent wave packets if these traverse the element's electrostatic field in regions of differing potential.

At very low electron energies (a few hundred eV), the longitudinal shift of the wave packets produced by the electrostatic fields along the beam path in our interferometer in general [26] exceeds by far the short coherence length available. This means that, without introducing an additional element compensating for this effect, no fringes at all are usually visible in the region of overlap.

IV. LONGITUDINAL COHERENCE RESTORING ACTION OF THE WIEN FILTER

A Wien filter is ideally suited as such a compensating element. In order to fulfill this purpose, its electric field has to be chosen of such a magnitude and direction that its action cancels the net longitudinal shift produced by all other electrostatic elements combined. The magnetic field per se has no influence on the longitudinal coherence, and its strength can therefore, in principle, be set to any arbitrary value. However, the Wien filter is usu-

ally (possible exceptions are mentioned below) operated in its matched mode; i.e., the magnetic field is chosen such that the magnetic force exactly cancels the electric force on the electrons [see Eq. (1)], thus yielding no net deflection of the beam. The salient point of this action by a Wien filter is then that both coherent partial beams traverse it (in a first-order approximation) on a rectilinear, transversally undeflected path, whereas they are longitudinally shifted relative to each other [see Figs. 2(b) and 2(c)]. This occurs because the partial beam that had been delayed in the deflection element(s) is given a higher group velocity in the Wien filter and vice versa. Figure 3 shows the combined effect of two electrostatic deflection elements used to compensate for a misalignment of the electron source, and the overlap-restoring effect of the Wien filter.

A series of micrographs of interference fringes (Fig. 4) illustrates the capability of a Wien filter to restore longitudinal coherence. The kinetic energy of the electrons was 358 eV, which corresponds to a de Broglie wavelength of 0.647 Å. With the Wien filter switched off, the fringe contrast was virtually zero (upper part of Fig. 4). In order to optimize the longitudinal coherence and thereby the fringe visibility in the observation plane, one has to increase the excitation of the Wien filter (while keeping it in matched mode) until the initial longitudinal shift—produced by all other electrostatic electron optical components—is exactly compensated by the Wien

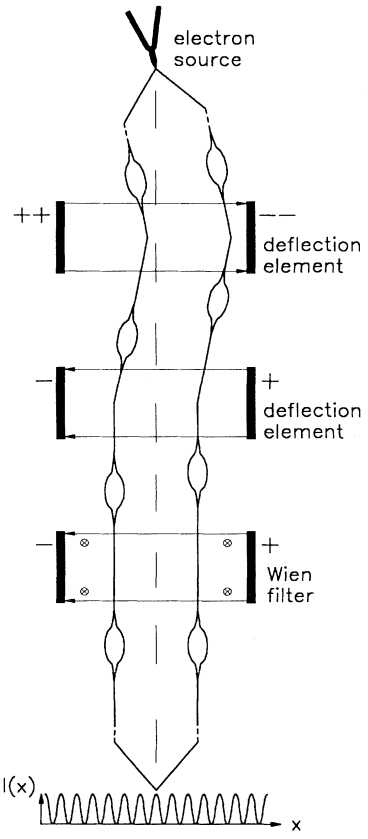

FIG. 3. Combined wave-packet-shifting effect of two deflection elements and a Wien filter. As an example, the electron source is slightly misaligned (the angular deviation is exaggerated in the drawing). The first deflection element bends the beams back toward the optical axis, and the second one makes them parallel again with the optical axis. Because the first deflection is approximately twice as large as the second one, the longitudinal shifts of the wave packets do not cancel out completely. The remaining spatial delay is eliminated by the Wien filter.

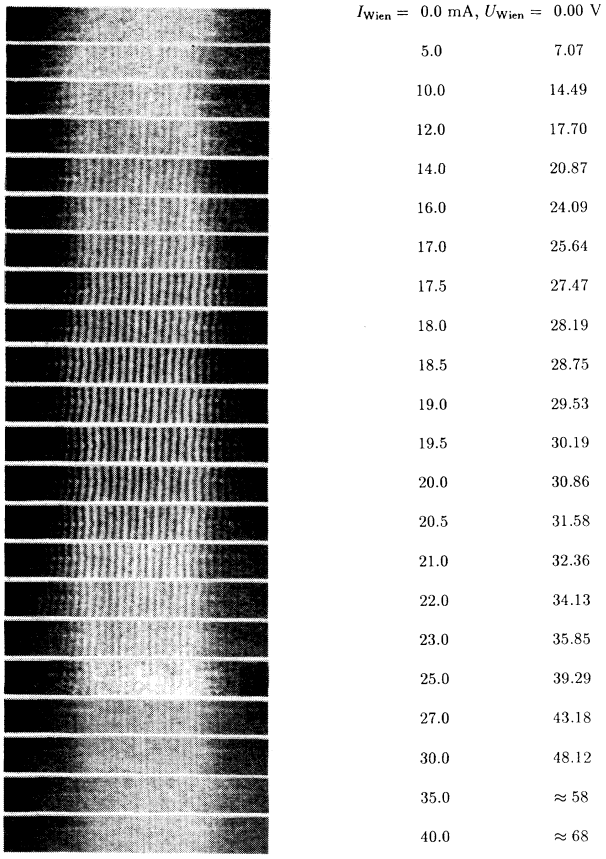

FIG. 4. Restoration of longitudinal coherence by a Wien filter. The excitation of the Wien filter increases from top to bottom. No fringes are visible at the top although the paths of the wave packets are accurately aligned to the optical axis of the interferometer. With increasing excitation, interference fringes appear, their contrast reaches its maximum (center), and disappears again when the compensating longitudinal shift produced by the Wien filter exceeds that caused by the electrostatic alignment elements (bottom). This set of micrographs was taken at an electron energy of 358 eV. On the right-hand side of each micrograph are given the values of the Wien filter excitation, i.e., the values of the current flowing through the coil generating the magnetic field, and the voltage applied to the Wien filter's deflection plates. (The last two voltage values are given only approximately because the end of the voltage range available for the Wien filter in this experiment had been reached, and an additional deflection element had to be used whose voltage could not be monitored exactly.)

filter. When full overlap of the wave packets in the interference plane is reestablished, maximum contrast of the interference fringes is attained (central part of Fig. 4). If the Wien filter is excited beyond that point, the longitudinal shift of the wave packets is overcompensated and the fringe contrast decreases and finally vanishes again (lower part of Fig. 4).

If we make the simplifying assumption that the spectral distribution of the field electrons has a Gaussian shape, we can derive an estimate of the coherence length from the contrast course in Fig. 4. If we equate the full width at half maximum (which is approximately 10 V) with U_d', i.e., the deflection voltage for which $\Delta y = l_c$ is fulfilled, we can derive l_c by entering the geometrical values of the Wien filter used in this experiment, $L = 5$ mm and $D = 8$ mm (see Fig. 2) in Eq. (7). With $\Delta x \approx 1$ μm, we obtain $l_c = 17$ nm. This is to be understood only as a rough estimate, since we neglected all complicating effects such as fringe fields, the detailed shape of the Wien filter's electrodes [12], the actual (not strictly Gaussian) shape of the field electron spectrum, and especially the uncertainty in the beam separation Δx stemming from the uncertainty in the determination of the biprism filament diameter [12]. This value of l_c clearly demonstrates the conservation of the coherence length along the beam path, since the geometrical spreading of the wave packets due to the dispersive propagation of electrons in vacuum yields much larger values for the "spread-out length" Δl of the wave packets. This can be easily estimated from the velocity spread corresponding to the energy spread of the field electrons of $\Delta U = 0.4$ V. With $\Delta l = l\Delta U/(2U_a)$ we obtain values of approximately 100 000 nm at the location of the Wien filter ($l = 177$ mm), and approximately 250 000 nm in the registration plane ($l = 440$ mm).

One might ask, at this point, about the possibility of spin-precession effects, caused by interaction of the magnetic moment of the electrons with the magnetic field of the Wien filter, to influence the results observed. Phase shifts due to spin precession are well known in neutron interferometry [27, 28] and, in principle, magnetic-field inhomogeneity or velocity differences over the two-beam paths could lead to phase gradients and washing out of the fringe visibility. If we ignore all other contributions to the Hamiltonian at the moment, it can be easily shown that from the Hamiltonian for an electron of momentum $\mathbf{p}$ and magnetic moment $\boldsymbol{\mu}$ traveling through a magnetic field $\mathbf{B}$,

$$H = \frac{p^2}{2m} - \boldsymbol{\mu}\cdot\mathbf{B}, \tag{19}$$

the phase shift to first order in $\mathbf{B}$ follows as

$$\beta = \pm 2\pi\mu_e BLm\lambda/h^2 \tag{20}$$

[27] if we assume a homogeneous magnetic field of length L. The $\pm$ signs stem from the two possible spin directions of the electrons relative to the magnetic field, and μ_e is the magnetic moment of the electron. The magnetic field (magnetic induction B) had been measured with a microprobe to be 3.4 mT at a current of $I = 100$ mA in a Wien filter of identical design. Assuming that the same B/I ratio was valid for the Wien filter used in the experiment described above, we estimate the maximum phase shift that occurred due to spin precession. At the Wien filter's maximum excitation, the Wien current was 40 mA, and for this value of I and for the values mentioned, $L = 5$ mm, $\lambda = 0.647$ Å, we obtain a total phase shift $\beta = \pm 0.85\%$ of one fringe period. This has to be compared to the total longitudinal shift that the wave packets have experienced relative to each other at the Wien filter's maximum excitation, which was approximately 116 nm, or approximately 1800 periods when expressed in phase units (although, as is shown below, no actual phase shift occurs to first order). The *total* phase shift caused by spin precession in the above experiment is therefore a 10^{-5} effect, and since β is a phase shift that both partial beams experience equally to first order (since they both travel through the same magnetic field), the *relative* phase shift between the two partial waves caused by field inhomogeneities and velocity differences [29] is much smaller still.

The following points pertaining to the action of the Wien filter are noteworthy.

(1) In its matched mode, the Wien filter does not exert a phase shift on the electron wave packets irrespective of its excitation, because the phase shifts caused by the two fields cancel exactly (in first-order approximation), as has been shown (see below) by Wohland [30]. Or, expressed in electron optical terms, a Wien filter operated in matched mode has an electron optical refractive index of 1. Two electron beams experience a phase shift relative to each other if they travel on paths with different optical path lengths $\int n\,ds$. Inversely, if n is constant and equal on both paths, no phase shift results. In analogy to light optics, the electron optical refractive index caused by the spatially varying electrostatic and magnetic potentials in an electron optical component is defined by [31]

$$n\left(\mathbf{r}, \frac{\mathbf{v}}{|\mathbf{v}|}\right) = \sqrt{\frac{\Phi(\mathbf{r})}{\Phi_0}} - \sqrt{\frac{e}{2mU_a}}\mathbf{A}(\mathbf{r})\cdot\frac{\mathbf{v}}{|\mathbf{v}|}. \tag{21}$$

Since the Wien filter is located after the acceleration of the electrons has taken place, the potential at the location of the Wien filter is $\Phi_0 = -U_a$. Since the electric field inside the Wien filter is assumed to be that of a parallel plate capacitor, we obtain $\Phi(\mathbf{r}) = Ex - U_a$ (in first-order approximation). We apply those relationships and expand the first term in (21) in x, which yields

$$\sqrt{\frac{\Phi(\mathbf{r})}{\Phi_0}} = \sqrt{1 - \frac{Ex}{U_a}} = 1 - \frac{Ex}{2U_a} + O(x^2). \tag{22}$$

The magnetic vector potential inside the Wien filter from which the applied magnetic field, $\mathbf{B} = (0, 0, B)$, follows is $\mathbf{A} = (0, Bx, 0)$. This gauge [in contrast to, e.g., $\mathbf{A} = (-By/2, Bx/2, 0)$] ensures that at both the entrance and the exit planes of the Wien filter the component A_x remains zero (otherwise the tangential component of $\mathbf{A}$ would become discontinuous at these planes and hence $\mathbf{B}$ would become infinite). Since we are analyzing the case of the Wien filter being in its matched mode, the

approximation that $\mathbf{v} = (0, v, 0) = \text{const.}$, i.e., that the electrons travel on an undeflected path through the entire Wien filter, holds to a very good degree. With this and with (21) and (22), we obtain

$$n = 1 - \frac{E\,x}{2U_a} - \sqrt{\frac{e}{2mU_a}}Bx + O(x^2). \tag{23}$$

Applying the Wien condition [Eq. (1)], $E = -Bv$, and employing $v = \sqrt{2U_a e/m}$, we find that the first-order terms in x cancel out, which leaves

$$n = 1 + O(x^2). \tag{24}$$

We have thus shown that, to first order in x, the two paths of the partial beams have the same electron optical path lengths, and that therefore no phase shift occurs in a Wien filter as long as the Wien condition is fulfilled. That this finding is in fact correct is shown by the observation that upon increasing the excitation of the Wien filter while keeping it in matched mode, only the contrast but not the position of the fringes in the interference pattern changes. This may be visualized in the somewhat unfamiliar picture of partial wave packets being shifted like [spindle-shaped; see Fig. 2(b)] windows in opposite directions along the beam path across a fixed (or "frozen") "phase wave sea."

(2) Due to the linear superposition that holds for the action exerted on electron wave packets by electric as well as by magnetic fields, the Wien filter does not necessarily have to be positioned behind all other electrostatic components in the beam path in order to exert its effect of restoring the longitudinal coherence. It may be positioned anywhere in the beam path, and may in fact even be the first component. One should, however, be aware of the fact that the effectiveness of the Wien filter depends on the separation Δx of the partial beams [see Eq. (7)] as they travel through its electric field. This separation usually changes along the beam path in an interferometer, thus often determining the optimum position of the Wien filter along the beam path for practical reasons.

(3) It follows immediately from the points made concerning its operating principle that the Wien filter does not even have to be constructed as one single-electron optical component. Its effect can be equally well produced by spatially separated electric and magnetic fields. In this case, however, the *deflections* caused by the two fields do not cancel locally, and have to be taken into account in the overall beam path.

(4) Although it is usually most practical experimentally to use the Wien filter in its matched mode, this is not a precondition for its coherence-restoring action (since, as we showed, the magnetic field itself does not exert a longitudinal shifting effect). It may in fact in special cases be desirable to obtain at the same time a deflection of the electron beams by the Wien filter.

(5) A Wien filter that is to be used for restoration of the longitudinal coherence in the way described in this paper necessarily poses very high demands on its voltage and current supplies in terms of stability. This can be easily shown by the following consideration. The total number of fringes in the interference field as given by the available coherence length [which is in most cases much larger than the number of *simultaneously observable* fringes, since this number is usually limited by the *spatial* (angular) coherence of the electron beam] is

$$N_c = \frac{l_c}{\lambda}, \tag{25}$$

and applying (11) to this immediately yields

$$N_c = a\frac{2U_a}{\Delta U}. \tag{26}$$

If we assume as typical values $U_a = 2000$ V, $\Delta U = 0.4$ V, and $a = 1$ (as a conservative choice, i.e., corresponding to only a partial loss of contrast), we obtain a total number of fringes of 10 000. If we believe that we *need* a Wien filter because a wave-packet shift of this magnitude, i.e., 10 000 fringe periods, or more, may occur in the interferometer, then we have to design the Wien filter and its voltage and current supplies in such a way that it will be able to exert a "counter-shift" of at least this magnitude—otherwise it would be useless. On the other hand, if the position of the interference fringes is to be measured with a precision of, e.g., 1% of a fringe period (for example, to determine a phase shift with this accuracy), then the relative stability of the Wien filter has to be at least 10^{-6} during the entire registration time, and this stability requirement has to be fulfilled by both the voltage and the current supply.

V. DISCUSSION

The effect of restoring coherence (and, for that matter, the operation of our interferometer in general) entails one striking characteristic that is not usually present in photon or neutron interferometry. In all electrostatic electron optical components, including the Wien filter, the electrons undergo continous energy exchanges with the environment (the electric fields). The energies exchanged vary from (approximately) equal values for both partial wave packets in potentials symmetrical to the optical axis, as, e.g., in the quadrupole lenses, to (approximately) opposite amounts $+\Delta E$ and $-\Delta E$ in potentials that are monotonous in the direction perpendicular to the beam paths, as, e.g., in the deflection elements. The energies that are exchanged in practice do easily, and often, reach nontrivial fractions of the kinetic energy in our interferometer. Take the example of two wave packets of 2-keV electrons separated by $\Delta x = 60$ μm (a value achieved in the Sagnac experiment [10]), propagating between two plates separated by $D = 5$ mm held at a potential U_d of +200 V and −200 V, respectively (values as high as these were often used in the experiments). The voltage difference ΔU_d experienced by the two wave packets being given by Eq. (5), we obtain $\Delta U_d = 4.8$ V (+2.4 V imparted to the one wave packet, −2.4 V to the other one). This corresponds to a relative energy difference between the two wave packets of 2.4×10^{-3} inside the deflection element. No observation in our interferometer, however, has ever indicated that this value would be a limit of any kind to the coherence conservation (or

the possibility of coherence restoration).

Evidently, this massive entanglement of the spatial (or center-of-mass) wave function with the environment does not *destroy* the coherence; however, it easily renders the coherence *"invisible,"* and it then takes a component such as a Wien filter to restore the visibility of the interference fringes.

This experimentally evident—but perhaps surprising—"robustness" of the quantum-mechanical coherence can easily be understood by considering the different conditions necessary for the actual observation of interferences. While the (potential) *occurrence* of interferences depends on the availability of two separate paths to the particles (so that an interference term occurs in the total, i.e., recombined, wave function that can be "scanned" for different values of the argument of this cosine term [32]), the *visibility* of the interference fringes additionally depends on the correct "arrangement" of the individual plane-wave components of the total wave function in the observation plane. These plane-wave components, as has been noted previously [6, 15], superpose incoherently for different wavelengths to form the observable interference pattern in the registration plane. This incoherent superposition is to be understood in the sense that the actual quantum-mechanical interference taking place is always the self-interference of a single-electron (but two-path) wave function. The single-particle regimen is practically always given in matter wave interferometry. In our interferometer, a typical electron energy of 2000 eV and a total path length of 44 cm from the electron source to the registration plane yield a flight time of 1.7×10^{-8} s. From a typical electron count in the observed interference region of 10^5 s^{-1} [33], we derive a typical average "duty cycle" of 1:600 for the electrons in the interferogram. The wave function describing this self-interference is that of the plane wave corresponding to the exact energy of this one electron [exact within the limits imposed by the uncertainty principle from the "life-time" of the electrons in the experiment (the above flight time), which yields an energy uncertainty on the order of 10^{-8} eV]. This plane-wave function is "infinite" compared to the coherence length of the wave packet, and even to its "spread-out length"; but of course it is in fact of the dimension of the interferometer since it is described by the Schrödinger equation (in the nonrelativistic case) with the boundary conditions given by the electron optical components and their fields.

The wave packet, then, is made out of such plane waves which have to have a well-defined spatial and energetic correlation so that their interference patterns (*intensities*) do not average out to zero fringe contrast when they add up in the observation plane. This correlation, which seems more akin to the classical coherence in light optics, is what is very easily destroyed in particle wave interferometry. In contrast hereto, the quantum-mechanical coherence of the self-interference of the particles' (plane-) wave functions seems very robust, and is in no way generally affected by, e.g., energy exchange with the environment.

In this picture, the various methods and experiments of reviving coherence (restoring contrast) in quantum-mechanical interferometry mentioned in the Introduction are then easily understood. When the plane-wave components have become "scrambled," and thereby fringe visibility lost, one can either "take out the bad ones," i.e., filter out part of the spectrum [14], or "bring them back in line," i.e., rearrange them so as to restore the correlation necessary for them to add up to visible fringes. This latter approach is the one we have taken by using the Wien filter. Of course a Wien filter is not capable of restoring just any loss of contrast, such as can be caused by other types of "inappropriate" overlap of the plane waves' interference patterns. These can, e.g., be caused by time-dependent (stray) fields, or by too large a source size (insufficient angular coherence). Of course, other kinds of filtering can be conceived (and have been used) to restore contrast in these cases.

VI. CONCLUSION

We have discussed the phenomenon of loss of fringe visibility caused by electric potential differences in charged-particle interferometry, and have described a way of restoring fringe contrast by using a Wien filter. If this is done by a Wien filter which is operated in matched mode, the unusual situation arises that no relative phase shift between the partial waves occurs, but only a longitudinal shift of the wave packets relative to each other. The possibility of restoring "lost" coherence shows that in particle interferometry, the quantum-mechanical coherence is not as easily truly destroyed as the experimental loss of fringe visibility sometimes suggests, but is often only "hidden" by effects such as the longitudinal shift described in this paper.

In conventional (high-energy) electron interferometers the wave-packet-shifting effect of electrostatic (alignment, etc.) fields has apparently not attracted attention so far because it leads only to a small decrease of the fringe contrast, due to the much larger coherence lengths there. However, for low-energy electron interferometers, the availability of a compensating element is of fundamental importance. It is also likely to be valuable in future ion-beam interferometers because of the even shorter coherence lengths encountered there.

---

* Present address: National Cancer Institute, National Institutes of Health, Bethesda, MD 20892.

† To whom correspondence should be addressed.

[1] H. Boersch, J. Geiger, and W. Stickel, Z. Phys. **180**, 415 (1964).

[2] E. Kisker, G. Baum, A. H. Mahan, W. Raith, and B. Reihl, Phys. Rev. B **18**, 2256 (1978).

[3] G. Möllenstedt and G. Wohland, in *Proceedings of the VIIth European Congress on Electron Microscopy, Den Haag, 1980*, edited by P. Bredoro and G. Boom (Seventh

European Congress on Electron Microscopy Foundation, Leiden, 1980), Vol. 1, p. 28.
[4] Strictly speaking, in this and the subsequently described application, we are not dealing with an (energy) *filter*, since this action requires the presence of additional beam stops. However, we adhere to the name Wien filter since it has been introduced in the literature, e.g., [3], even for this type of application.
[5] I. Daberkow, H. Gauch, and F. Hasselbach (unpublished).
[6] F. Hasselbach and A. Schäfer, in *Proceedings of the 12th International Congress for Electron Microscopy, Seattle, 1990*, edited by L. D. Peachey and D. B. Williams (San Francisco Press, Inc., San Francisco, 1990), Vol. 2, p. 110.
[7] H. Kaiser, S. A. Werner, and E. A. George, Phys. Rev. Lett. **50**, 560 (1983).
[8] F. Lenz and G. Wohland, Optik (Stuttgart) **67**, 315 (1984).
[9] F. Hasselbach and M. Nicklaus, Physica B **151**, 230 (1988).
[10] F. Hasselbach and M. Nicklaus, preceding paper, Phys. Rev. A **48**, 143 (1993).
[11] F. Hasselbach, Z. Phys. B **71**, 443 (1988).
[12] M. Nicklaus, Ph.D. thesis, University of Tübingen, Germany, 1989.
[13] R. Clothier, H. Kaiser, S. A. Werner, H. Rauch, and H. Wölwitsch, Phys. Rev. A **44**, 5357 (1991).
[14] S. A. Werner, R. Clothier, H. Kaiser, H. Rauch, and H. Wölwitsch, Phys. Rev. Lett. **67**, 683 (1991); H. Kaiser, R. Clothier, S. A. Werner, H. Rauch, and H. Wölwitsch, Phys. Rev. A **45**, 31 (1992).
[15] H. Rauch, H. Wölwitsch, R. Clothier, H. Kaiser, and S. A. Werner, Phys. Rev. A **46**, 49 (1992).
[16] H. Rauch, Phys. Lett. A **173**, 240 (1993).
[17] A. G. Klein, G. I. Opat, and W. A. Hamilton, Phys. Rev. Lett. **50**, 562 (1983).
[18] A. M. Steinberg, P. G. Kwiat, and R. Y. Chiao, Phys. Rev. Lett. **68**, 2421 (1992); Phys. Rev. A **45**, 6659 (1992).
[19] P. G. Kwiat, A. M. Steinberg, and R. Y. Chiao, Phys. Rev. A **45**, 7729 (1992).
[20] G. Möllenstedt and H. Düker, Naturwissenschaften **42**, 41 (1955).
[21] G. Möllenstedt and H. Düker, Z. Phys. **145**, 377 (1956).
[22] G. W. Fraser, Nucl. Instrum. Methods **206**, 445 (1983).
[23] K.-H. Herrmann and M. Korn, J. Phys. E **20**, 177 (1987).
[24] Normally, i.e., if only one biprism is used, Δx is on the order of the biprism filament diameter of typically 1 μm. In the Sagnac experiment [10], however, where multiple biprisms were used, Δx could be as large as 60 μm.
[25] M. Born and E. Wolf, *Principles of Optics*, 2nd ed. (Pergamon, Oxford, 1964), p. 316.
[26] After fine alignment of the electron beams to the optical axis, no fringe contrast is usually observed, unless all wave-packet-shifting influences combine by pure coincidence to a net relative delay smaller than the coherence length.
[27] S. A. Werner, R. Collela, A. W. Overhauser, and C. F. Eagen, Phys. Rev. Lett. **35**, 1053 (1975).
[28] H. Rauch, A. Zeilinger, G. Badurek, A. Wilfing, W. Bauspiess, and U. Bonse, Phys. Lett. **54A**, 425 (1975).
[29] The velocity differences that are relevant in this context are caused by the electric potential of the Wien filter. As is shown in Sec. V, the relative velocity differences reached can be nontrivial from a fundamental point of view, but are nevertheless typically on the order of 10^{-3} or less. In this experiment, they were approximately 4×10^{-5}, and multiplying this by the total phase shift caused by spin precession of 0.85% of a fringe period obviously yields a totally negligible effect.
[30] G. Wohland, Ph.D. thesis, University of Tübingen, Germany, 1981.
[31] W. Glaser, Z. Phys. **80**, 451 (1933).
[32] This usually happens simultaneously in electron biprism interferometers, where the overlap angle $\gamma > 0$ generates the phase differences through the slightly different path lengths leading to the different positions in the observation plane; whereas in (single-) photon and in neutron interferometry, the usual overlap angle of zero forces one to do this "scanning," e.g., by subsequent, stepwise path-length variation in one arm of the interferometer.
[33] One could argue that the total emission current was much higher, with typical values in the 10–1000-nA range (10^{11}–10^{13} s^{-1}). However, due to beam stops, etc., only a small part of these electrons reaches the observation plane. Furthermore, it was possible to reduce the emission current to extremely low values of maybe a few thousand electrons per second, and still observe exactly the same effects as at higher currents. Such very low currents are merely difficult to handle experimentally.

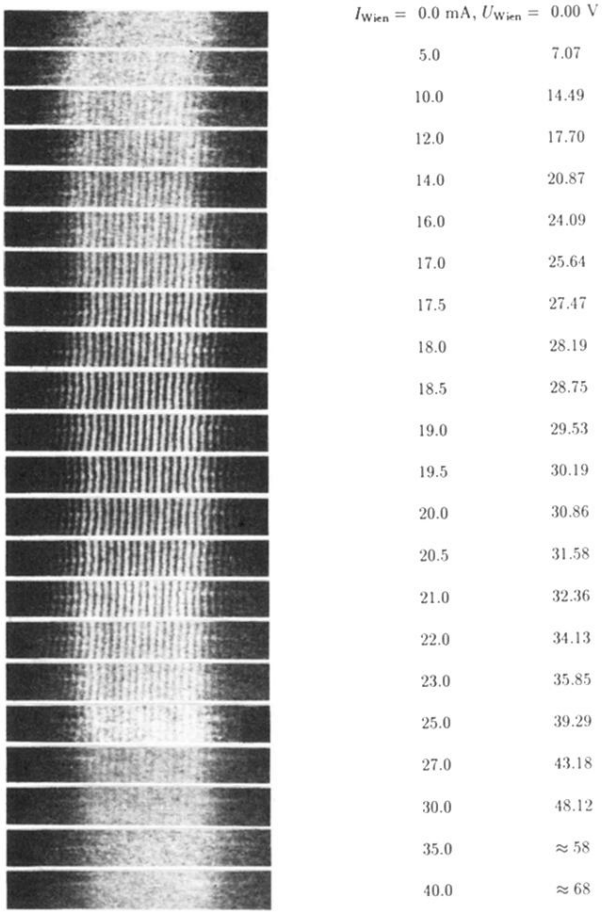

FIG. 4. Restoration of longitudinal coherence by a Wien filter. The excitation of the Wien filter increases from top to bottom. No fringes are visible at the top although the paths of the wave packets are accurately aligned to the optical axis of the interferometer. With increasing excitation, interference fringes appear, their contrast reaches its maximum (center), and disappears again when the compensating longitudinal shift produced by the Wien filter exceeds that caused by the electrostatic alignment elements (bottom). This set of micrographs was taken at an electron energy of 358 eV. On the right-hand side of each micrograph are given the values of the Wien filter excitation, i.e., the values of the current flowing through the coil generating the magnetic field, and the voltage applied to the Wien filter's deflection plates. (The last two voltage values are given only approximately because the end of the voltage range available for the Wien filter in this experiment had been reached, and an additional deflection element had to be used whose voltage could not be monitored exactly.)